2.3.2 Physics of CFD Solver - RANS

The RANS solver is used for CFD analysis throughout this dissertation as it is the most accurate method for the time and computational resources available. The aim of the RANS solver is to solve the Reynolds Averaged Navier-Stokes equations as set out below.

$$\frac{\partial \bar{u}_i}{\partial x_i} = 0$$

$$\frac{\partial \bar{u}_i}{\partial t} + \bar{u}_j \frac{\partial \bar{u}_i}{\partial x_j} = -\frac{1}{\rho}\frac{\partial \bar{p}}{\partial x_i} + \frac{\partial}{\partial x_j}\left(\nu \frac{\partial \bar{u}_i}{\partial x_j} - \overline{u_i' u_j'}\right)$$

This equation contains the $\overline{u_i' u_j'}$ term which represents the 6 components of the Reynolds Stress and so introduces an additional 6 unknown variables as opposed to the single unknown before the Reynolds Averaging process was applied to the Navier-Stokes equations. To solve for the Reynolds Stress a turbulence model must be used to close the equation set. The most common method for this is to use an Eddy Viscosity/Boussinesq model. An Eddy Viscosity turbulence model introduces a Turbulent Viscosity variable (ν_T) that is a function of the flow, not the fluid, and is used to close the equation set by defining the relationship between the

turbulence and the mean flow. One downfall of the Eddy Viscosity method is that it results in a scalar eddy viscosity (isotropic) when in actual fact it is a tensor and the turbulence is non-isotropic. Non-Eddy Viscosity models (tensor) can also be used to close the equation set and are much more accurate but many times more computationally expensive and so are not commonly used and require a much more refined grid to accurately resolve the turbulence in all directions without diverging.

2.3.3 Mesh Requirements - RANS

To solve the flowfield the solver requires a discretised domain. The domain must first be generated in a software package such as Pointwise Gridgen and include the geometry that is to be analysed and the relevant external domain or internal details. There are numerous ways to discretise the domain and each has a different effect on the solver and the accuracy of the results. The mesh generation process is critical to obtaining a CFD result that is comparable to

3.4 Oil Flow Visualisation

3.4.1 Clean Wing

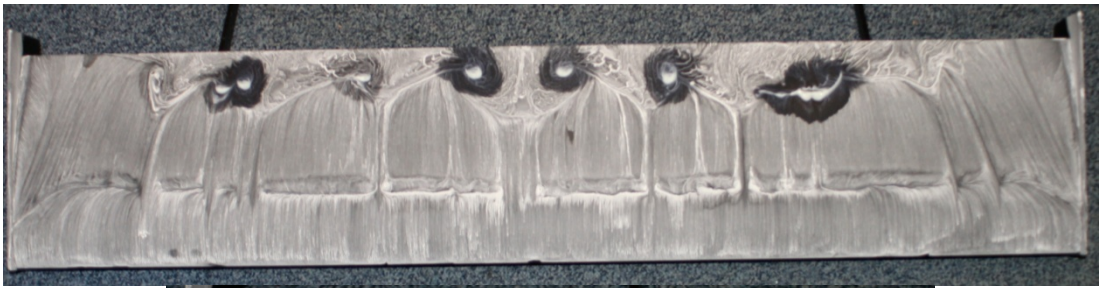

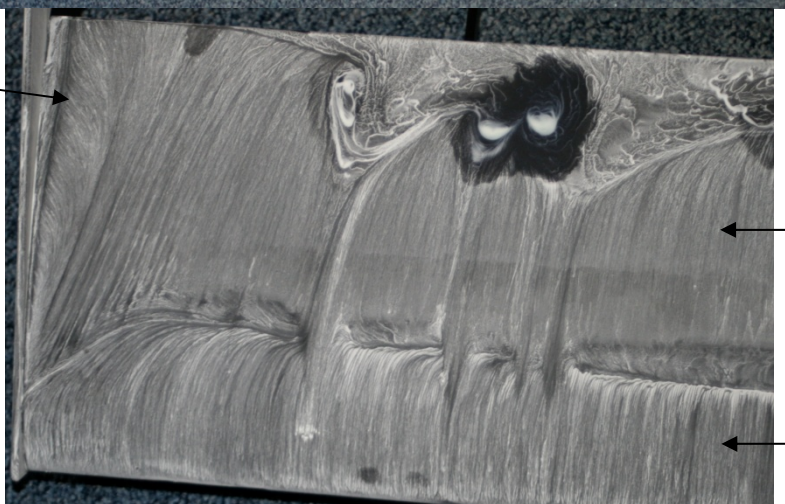

Figure 3.14 - Oilflow Visualisation - Clean Wing Complete and Edge

The above image and Figure 3.15 show the resultant particle distribution on the surface of the Clean Wing from a run at h/c = 0.09 and 1 degree angle of attack. This residual flow visualisation shows that the wing profile was designed with a separation bubble along the span of the wing. This design feature is included to trip the boundary layer from laminar to turbulent so that the profile can further resist separation. This effectively fixes the transition point of the wing. However, there are some sections where the fluid passes through the designed separation bubble and laminar flow is retained until further downstream on the wing surface. A large separation region exists at the trailing edge of the wing and it appears to separate into regions of vortical flow. An edge vortex is present at the extremities of the wing and this provides the additional energy to withstand separation towards the wing tips.

The previous plots show the convergence of C_L and C_D. It can be seen that these results are converging to a steady solution as the number of iterations is increasing. Noting the scale on the side we can see that the values are converging with a relatively small change in results.

After checking for Coefficient of Lift and Drag convergence for each simulation, the following results were plotted for the various turbulence models. It is clearly seen that the Spalart-Allmaras turbulence model has the most representative result to the Experimental Data that has been obtained.

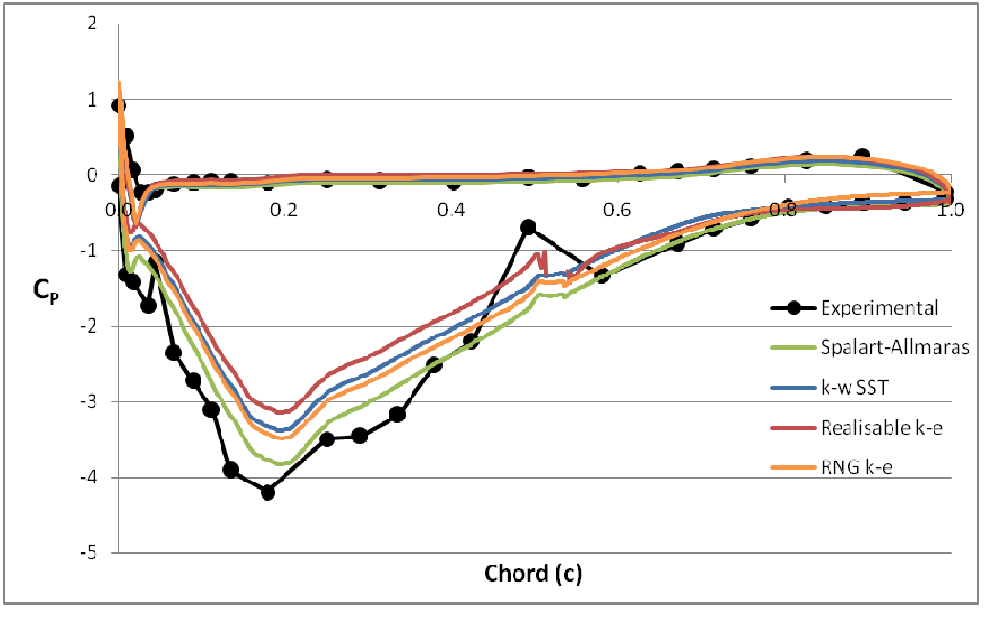

Figure 4.8 - C_p Plot of Alternate Turbulence Models - Co Rotating SVG Wing

The choice of turbulence model that appears best from the pressure distribution (Spalart-Allmaras) is also reflected in the force results shown below. The C_L and C_D Error are the closest to the Experimental data for the Spalart-Allmaras model, although closely followed by the RNG k-e model.

	C_L	C_D	C_L Error	C_D Error	Iterations
Spalart-Allmaras	-1.6470	0.0653	1.79	-9.20	53000
k-w SST	-1.4241	0.0613	-11.98	-14.87	62000
Realisable k-e	-1.4872	0.0932	-8.08	29.49	65000
RNG k-e	-1.5367	0.0694	-5.02	-3.58	76000
Reynolds Stress Model	Would not Converge				
Experimental	-1.6180	0.0720	0.00	0.00	

Table 4.5 - Force Results for Alternate Turbulence Models - Co Rotating SVG Wing